2. LEG 8 SUMMARY[1]

Shipboard Scientific Party[2]

SETTING

The equatorial Pacific has long been recognized as an area of high productivity and high standing crops of plankton (Graham, 1941; Cromwell, 1953; Ryther, 1963). The divergence of surface waters at the equator and the shallow thermocline at the northern edge of the Equatorial Counter-current bring nutrient-rich, deeper waters into the near surface habitat of phytoplankton (Figure 1). The resulting latitudinal bands of high phytoplankton productivity apparently sustain a high standing crop of zooplankton, the combined volume distribution being similar to the nutrient distribution shown in Figure 1 (Reid, 1962).

The pelagic sediments beneath such regions of high productivity are composed primarily of the calcareous and siliceous tests of planktonic organisms. Since the original Challenger expedition in the 1870's, it has been known that a broad equatorial band of highly fossiliferous sediments exists in the Pacific. Reflection profiler records show that an elongate mound of sediments (Figure 2) stretches from the eastern Pacific westward to the Line Islands centered about two degrees north latitude (Ewing *et al.*, 1968). Near the equator, samples of the near-surface sediments are rich in carbonate skeletal material (Figure 3; Bramlette, 1961), but to the north and south (at the fringes of the high productivity zone) the relative proportion of carbonate gradually decreases until the sediments contain only the siliceous skeletons of Radiolaria, silicoflagellates and diatoms. At higher latitudes, sparsely fossiliferous "red clays" are found beneath the relatively barren central water masses.

The carbonate-rich surface sediments along the equator are usually Quaternary in age, but sediments of Tertiary age are commonly sampled a few degrees north and south of the equator (Hays *et al.*, 1969), and increasingly older surface sediments are likely to be encountered at progressively higher latitudes (Riedel and Funnell, 1964). There is also evidence that the

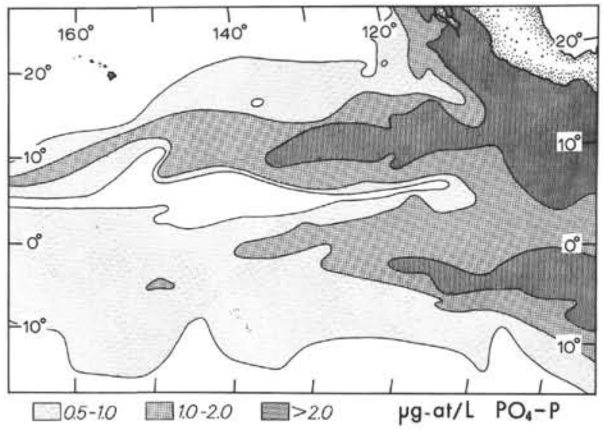

Figure 1. *Concentration of phosphate-phosphorus at 100-meter depth in waters of the equatorial Pacific (after Reid, 1962).*

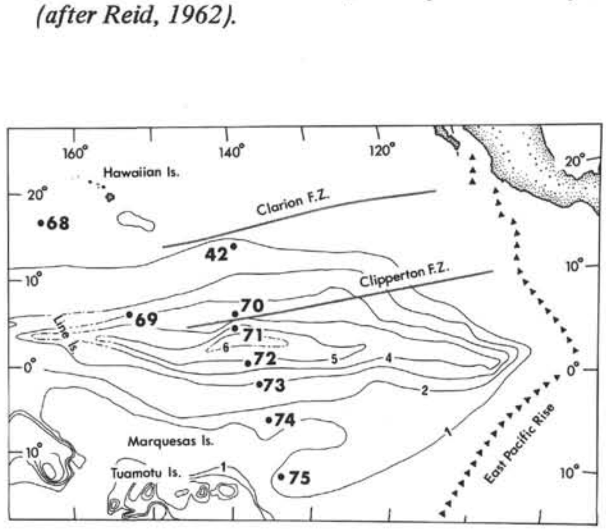

Figure 2. *Sediment isopach map of the equatorial Pacific. Numbered contours represent tenths of seconds reflection time from the sea floor to the acoustic basement (modified after Ewing* et al., *1968). Leg 8 (Sites 68 through 75) and Leg 5 (Site 42) site locations indicated by dots.*

[1]Publication authorized by the Director, U. S. Geological Survey.

[2]Joshua I. Tracey, Jr., U. S. Geological Survey, Washington D. C.; George H. Sutton, University of Hawaii, Honolulu, Hawaii; W. D. Nesteroff, Université de Paris, Paris, France; Jon Galehouse, San Francisco State College, San Francisco, California; C. C. von der Borch, Scripps Institution of Oceanography (present address: Flinders University, Bedford Park, South Australia); T. C. Moore, Oregon State University, Corvallis, Oregon; U. Z. Bilal ul Haq, Geologiska Institutionene, Stockholm, Sweden (present address: Woods Hole Oceanographic Institution, Woods Hole, Massachusetts); and J. P. Beckmann, Geologisches Institute, Zurich, Switzerland.

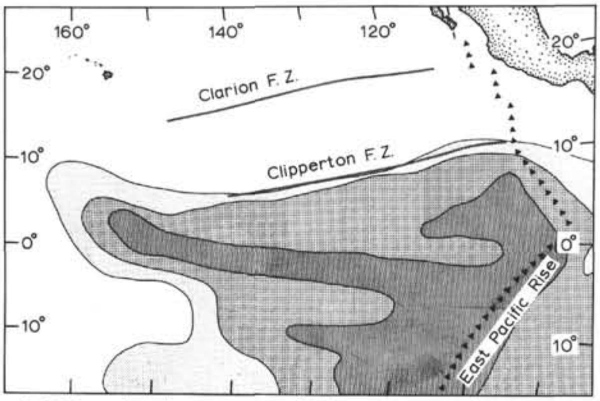

Figure 3. *Concentration of calcium carbonate in surface sediments of the equatorial Pacific (after Bramlette, 1961).*

proportion of calcium carbonate preserved in equatorial sediments fluctuated during the Late Cenozoic and that a broader equatorial zone of calcareous and siliceous deposition existed during the early Cenozoic (Arrhenius, 1963).

LITHOLOGY

Sites 70 through 75, together with Site 42 of Leg 5 (McManus *et al.*, 1971) form a nearly north-south section across the equatorial mound of sediments (Figure 4). The sediments are composed almost entirely of biogenic deposits of calcareous and siliceous ooze, diagenetically altered to limestone and chert in some of the older portions of the section. Red clay, zeolites, volcanic ash and shards, and amorphous iron oxides are locally abundant in some samples but are volumetrically insignificant.

Three major lithologic units are here designated oceanic geologic formations. They are: the Line Islands Oceanic Formation–a lower unit of Eocene age consisting of semi-indurated radiolarian ooze, calcareous ooze, silicified limestone and chert. This is overlain with marked disconformity by the Marquesas Oceanic Formation–a homogeneous middle unit of predominantly white highly calcareous nannofossil ooze, of Oligocene and Miocene age. The Marquesas is in turn overlain by the Clipperton Oceanic Formation–a heterogeneous upper unit of Miocene to Holocene age consisting of radiolarian ooze, of cyclically bedded calcareous and siliceous ooze, and of light colored highly calcareous ooze containing purple, green and blue-gray bands or beds (Figure 4).

The three pelagic sedimentary units were deposited during successive episodes of the Cenozoic under the influence of three apparently distinctive oceanographic regimes. Site 70, at 6° 20′N, 140° 22′W, (Figures 2 and 4) is designated the type section for each of the three formations[3], although some subunits or facies, especially of the upper formation, are better developed at other sites. Sites 42, 69 and 71 through 75 are designated reference sections. The depths and thicknesses of the formations and their subunits at each site are shown in Table 1, and a diagrammatic sketch (Figure 5) shows the relations of the formations along this stratigraphic section. Detailed descriptions of the sediments and fossils are given in Site Reports (Part 2) in this volume.

These formational names apply in the depositional basin where they are defined–bounded generally by the East Pacific Rise, the Line Islands (Christmas Ridge), the Tuamotu and Marquesas Ridges, and the Clarion Fracture Zone–unless their continuity into adjacent basins can be demonstrated by mapping and coring.

Line Islands Oceanic Formation

The lowermost unit is here named for the Line Islands that form a western limit to the sedimentary basin. The type section is Site 70, 324 to 388 meters below the sea floor; Sites 42, 69 and 71 through 74 are reference sections (see Site Reports). The formation consists of semi-indurated brown radiolarian ooze; yellowish-brown rather siliceous calcareous nannofossil ooze; greenish-gray laminated siliceous to cherty limestone; and black, brown, red and gray chert containing traces of foraminifera and Radiolaria. The semi-indurated ooze is predominant in the upper part of the unit, which is of late Eocene age, whereas limestone and chert are more extensive in the lower part of the unit, which is of middle Eocene age. Because of the lithification, much of the unit was drilled rather than cored. In most holes drilling and coring stopped in chert; little is known of the thickness or the nature of the basal contact of the formation. The formation was completely penetrated only at Site 74, where it is about 2 meters thick and consists of calcareous ooze containing zeolites and amorphous iron oxides overlying basalt. The formation pinches out to the south and was not present at Site 75. More than 80 meters are present at Site 42 (McManus *et al.*, 1971) and more than 87 meters at Site 69. The upper boundary is a marked disconformity. The varicolored semi-indurated

[3]We follow the code of the American Commission on Stratigraphic Nomenclature (1961) rather than the recommendation of Andrews and Hsu (1970) for formation names and type sections. In order to develop a uniform nomenclature for this region, Harry Cook, of the Leg 9 staff, made a cooperative examination of logs and strip photographs of Leg 8 and Leg 9 cores with Jon Galehouse of Leg 8.

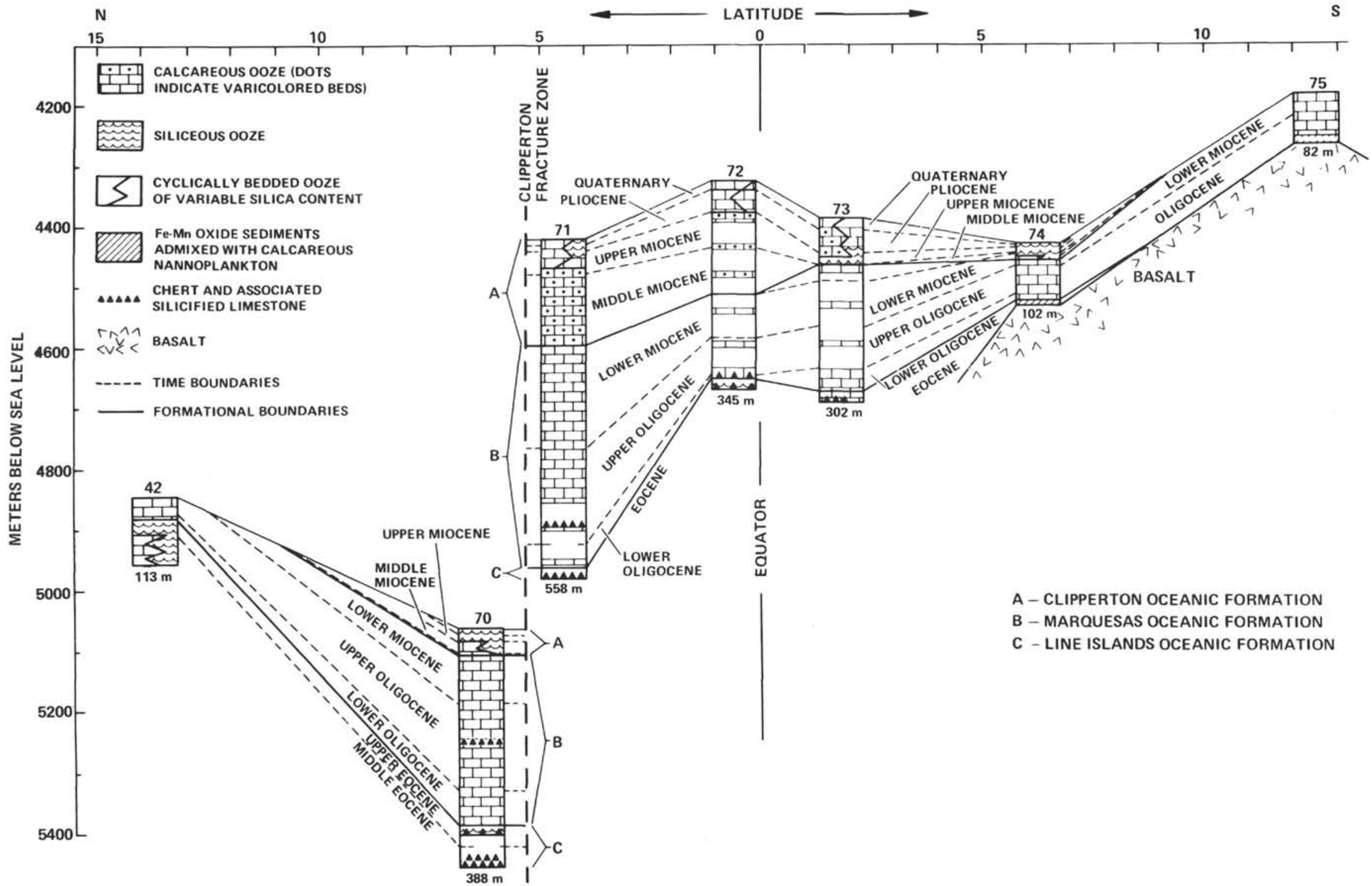

Figure 4. *Stratigraphic section along 140°W, showing lithology, time-stratigraphic correlations, and oceanic formational units. Location of sections shown in Figure 2.*

TABLE 1
Depth and Thickness of Oceanic Formations

Site	Formation Unit	Depth (meters)	Thickness (meters)	Contact
42	Marquesas	0-32	32	Sharp
	Line Islands	32-113	81	
69	Clipperton	0-35	35	
	Radiolarian ooze	0-19.6	20	Sharp
	Cyclic	19.6-35	15	Uncored
	Marquesas	35-144	109	Sharp
	Line Islands	144-231	87	
70	Clipperton	0-45	45	
	Radiolarian ooze	0-19.8	20	Sharp
	Cyclic	19.8-45	25	Sharp
	Marquesas	45-323.7	279	Sharp
	Line Islands	323.7-388	64	
71	Clipperton	0-188	188	
	Cyclic	0-43	43	Sharp
	Varicolored	43-188	145	Gradational
	Marquesas	188-545	357	Uncored
	Line Islands	545-558	13	
72	Clipperton	0-180	180	
	Cyclic	0-34.5	35	Sharp
	Varicolored	34.5-180	145	Uncored
	Marquesas	180-339	159	Sharp
	Line Islands	339-345	6	
73	Clipperton	0-73.4	73	
	Cyclic	0-6.5	7	Sharp
	Varicolored	6.5-62.9	56	Mixed
	Radiolarian ooze	62.9-73.4	10	Sharp
	Marquesas	73.4-288	215	Sharp
	Line Islands	288-302	14	
74	Clipperton	0-23.5	24	
	Radiolarian ooze	0-23.5	24	Sharp
	Marquesas	23.5-100	76	Sharp
	Line Islands	100-102	2	Sharp
	Basalt			
75	Residuum	0-1.3	1	Sharp
	Marquesas	1.3-82	81	Sharp
	Basalt			

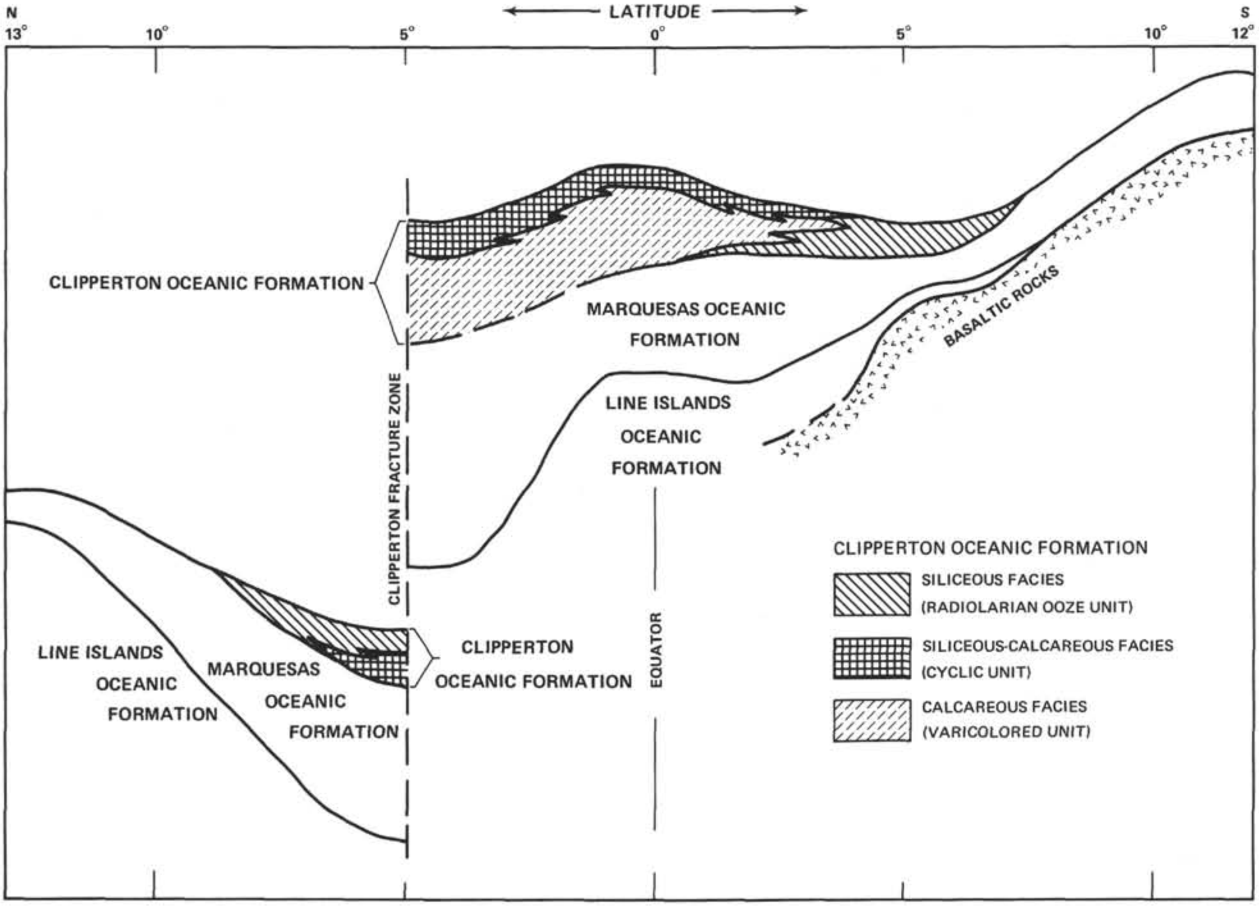

Figure 5. *Diagrammatic sketch of equatorial sediments at about 140°W longitude. Clipperton Oceanic Formation: A – siliceous facies (radiolarian ooze unit); B – siliceous-calcareous facies (cyclic unit); C – calcareous facies (varicolored unit).*

Line Islands Oceanic Formation is overlain by white highly calcareous nannofossil ooze of the Marquesas Oceanic Formation.

Marquesas Oceanic Formation

The middle unit is here named for the Marquesas Islands; the type section is designated as Site 70, 45 to 324 meters below the sea floor. Sites 42 (McManus *et al.*, 1971), 69, and 71 through 75 are reference sections (see Site Reports). The unit is composed of white highly calcareous ooze made up chiefly of calcareous nannofossils. Foraminifera are also common calcareous fossils, and radiolarians are the chief siliceous contributors. The bulk of the formation is white or off-white almost everywhere except at the southern Sites 74 and 75 where it is light to moderate yellowish-brown. It generally contains 80 to 95 per cent or more calcium carbonate ($CaCO_3$) and rarely less than 60 to 70 per cent. Where it is very thick, the lower part of the formation is firm to chalky and contains a few scattered nodules and stringers of chert (Sites 70, 71 and 72).

Along the line of the drilled section, the Marquesas ranges in thickness from about 300 meters near the Clipperton Fracture Zone to about 30 meters at Site 42 (latitude 12° 52′N), and 80 meters at Site 75 (12° 31′S). It apparently thins and pinches out further north and south, and it thins and becomes more siliceous to the west (Site 69). The thickness and extent of the Marquesas eastward toward the crest of the East Pacific Rise will have to be determined by study of the subsequent drilling by Leg 9.

The Marquesas Oceanic Formation overlies the Line Islands Oceanic Formation disconformably in most of the drill holes, but it overlaps the Line Islands and overlies basaltic rock to the south (Site 75). The upper boundary of the formation is its contact with the overlying Clipperton Oceanic Formation, which is gradational at Sites 71, uncored at Sites 69 and 72, but is sharp at Sites 70, 73 and 74. Where the Clipperton is not present, as at Sites 42 and 75, the upper boundary of the Marquesas is the sea floor, or a thin layer of mixed residuum that might be compared to a soil zone on land.

The age of the Marquesas is Oligocene and Miocene. Its base is in the lower Oligocene along the longitudinal section (Sites 42 through 75) and at Site 69. The top of the Marquesas is near the top of the Oligocene at Site 42, within lower Miocene sediments at Sites 69, 70, 74 and 75, and about at the top of middle Miocene at Site 73. It is about at the top of the lower Miocene at Site 71 where it grades into a high-carbonate facies of the overlying Clipperton, and possibly also at Site 72, where the contact was not cored.

Clipperton Oceanic Formation

The uppermost unit is here named for the Clipperton Fracture Zone which is situated south of the designated type section (Site 70, 0 to 45 meters). Sites 69 and 71 through 74 are reference sections (see Site Reports). The Clipperton contains pelagic sediments of three lithologic types whose distribution in the drill holes suggests that they may be mappable as informal members within the Clipperton. They are: (1) Brown radiolarian ooze, highly siliceous, up to 24 meters thick, that forms much of the Clipperton Oceanic Formation at Sites 69 and 70, at about 6°N, and Site 74, at about 6°S. A 10-meter layer is found at the base of the Clipperton at Site 73. (2) A cyclically or rhythmically bedded unit of orange to white highly calcareous nannofossil ooze containing siliceous beds of pale brown to dark brown beds rich in Radiolaria. The unit is dominantly siliceous with calcareous beds at Site 69, where it forms the lower part of the Clipperton. It is predominantly calcareous with thin, pale brown, more siliceous beds at Site 70, where it forms the lower part, and at Sites 71 and 73, where it forms the upper part of the Clipperton. (3) A very light, varicolored unit of highly calcareous nannofossil ooze at Sites 71, 72 and 73. At Sites 71 and 72 the sediment is predominantly white calcium carbonate, apparently homogeneous in carbonate content as is the underlying Marquesas Oceanic Formation, but it contains bands or beds of pale purple, green and blue. The thick varicolored unit is compositionally close to the Marquesas. It is transitional into the overlying cyclic unit of the Clipperton, and is assigned to the Clipperton rather than to the more homogeneous Marquesas because of its bedded or rhythmic character.

The Clipperton ranges in thickness from about 180 meters at Sites 71 and 72, where it is predominantly calcareous, to 45 meters at Site 70, 35 meters at Site 69, and 24 meters at Site 74, where it is highly siliceous and the calcareous components are largely dissolved. It apparently pinches out by about 10°N and 10°S. The Clipperton overlies Marquesas at all Leg 8 sites where it was present. The lower contact of the Clipperton Oceanic Formation is gradational in Hole 71, and probably in Hole 72 where it was not cored, and is about at the top of the lower Miocene. At Sites 69, 70 and 74 the contact is sharp and within the lower Miocene at about the N. 5 Foraminiferal Zone (see Beckmann report, this volume). At Site 73 it is sharp and at about the top of the middle Miocene. The upper boundary of the Clipperton is the sea floor.

Relations of the Formations

A diagrammatic sketch (Figure 5) shows relations of the formations across the equator. A disconformity, apparently regional in extent, separates the Line Islands from the Marquesas Oceanic Formations. The Marquesas sediments are characterized by their relative homogeneity in composition and color, indicating uniform conditions of deposition over a broad region. Clipperton sediments are characterized by increasing silica content on both the north and south margins of the formation, by cyclic changes in silica content of the more calcareous beds, and by the presence of varicolored beds in the central highly calcareous part of the formation, chiefly in the middle Miocene at Site 71, the upper Miocene at Site 72, and the Pliocene at Site 73.

The contact between Clipperton and Marquesas Oceanic Formations is sharp at the north and south margins, but is gradational at Sites 71 and 72. It is apparently unconformable at Site 73, as indicated by a transgressive shallow reflection horizon in the seismic reflection records, but the unconformity may be relatively local in extent.

Lithification of Sediments

The degree of induration of the pelagic oozes at all sites seems to be related to age of the sediments and to depth of burial. No induration was found within the Clipperton except for a few chert chips at the top of Core 19 at Site 71, at a depth of 162 meters.

The calcareous nannofossil ooze of the Marquesas Oceanic Formation is semi-indurated to the consistency of a chalk only at Sites 70, 71 and 72. At Site 70 the chalklike consistency occurs below a thin (6 centimeter) chert at about 190 meters below the sea floor. At Site 71 the ooze is firm enough to require use of the pump in coring below about 200 meters, but is chalky only below the first significant chert (3 centimeters) in Core 49 at 470 meters. Core 71A-1 at 530 meters, near the base of the Marquesas, is indurated nearly to a limestone. At Site 72, the nannofossil ooze is firm below a chert layer at 312 meters. At all three sites the chert at the top of the semi-indurated ooze (chalk) occurs within the P. 21 Foraminiferal Zone, which is of late Oligocene age.

Although the world wide development of chert and siliceous limestone in sediment of Eocene age is well known, it is difficult to establish the time and the conditions which led to the lithification in this region, because so few cores were taken in Eocene rocks, and because relatively little hard rock was penetrated. Chert layers and limestone appear to be more extensive in rocks of middle Eocene than of late Eocene age, but they are also apparently most lithified at Sites 70 and 71 (which only penetrated the top of the late Eocene) where they are most deeply buried. The Eocene sediments of Site 42 are reported by McManus and others (1971) to be firm radiolarian ooze of late and middle Eocene age from a depth of 32 meters to about 100 meters, below which limestone and chert fragments were recovered along with the ooze. At Site 68, however, in deeper water (5466 meters) brown clay of middle Eocene age contained thin siliceous and cherty layers starting only 9 meters below the sea floor. A more detailed description of the chert and limestone are given by von der Borch and others in Part III of this volume.

PHYSICAL PROPERTIES

Given in Figures 6 through 8 are smoothed plots of sonic impedance (bulk density times sonic velocity), sonic velocity, and penetrometer reading versus depth for Sites 69 through 75. More detailed plots of these parameters along with plots of bulk density, porosity, and grain-matrix density are included in each site report, Chapters 3 through 10. In general, these plots indicate a decrease in porosity and an increase in stiffness with depth in the sediment column as might be expected from gravitational compaction and partial lithification. However, the general trend is complicated by changes in lithology, principally from highly calcareous to highly siliceous ooze, and by lithified zones in deeper portions of the sediment section at some of the sites. (Measurements on indurated samples are not included in the plots. They are discussed separately below.)

The possible effects of drilling and recovery procedures on the measured physical properties are not well understood. For the sediments encountered on Leg 8, we believe most of the measurements are fairly representative of *in situ* values. Obvious water-filled breaks in the core were not measured; also excluded were sections apparently fluidized during drilling or coring. It seems about equally difficult for fluid to be uniformly inserted into the sediment, increasing the porosity, as for it to be squeezed out, decreasing porosity. Sonic velocity for unlithified sediments such as those encountered is controlled mainly by the porosity; laboratory measurements of velocity should be representative of *in situ* values provided the porosity was not modified significantly. Using interval velocities between intermediate reflectors as measured on cores in the laboratory, depth of the acoustic basement in general agrees well with that for the lithified sediments or basalt encountered at the bottom of the holes. However, it should be noted that fairly good correlation might be obtained for most of the sites using a higher average velocity (about 1.7 km/sec) for the sediments. This change would not appreciably affect the shallower sites, but would require different (somewhat less likely) arguments regarding the contributions of local structure and the reflectivity of the indurated chalk and chert near the base of the section at Site 71. Disturbance might have reduced sediment rigidity and increased penetrability. However, the observed general decrease in penetrometer readings with depth indicates that this effect might not be serious for most of the sections measured.

In Figure 7 sonic velocity in the sediment at laboratory temperature and pressure is compared with that in sea water, measured in the laboratory under the same conditions. Provided the sediment velocities are representative of *in situ* values, the data for most of the sites indicates that a fairly thick "low-velocity channel" exists within the sediments, with the minimum velocity occurring at a depth between 30 and 100 meters below the sea floor. The average velocity within the sediments is quite low for such thick sections returning back up to velocity of sea water at depths as great as 200 meters below the sea floor. Site 75 is an exception to the above remarks. There, the porosity decreases rapidly with depth and the velocity rises to exceed water velocity at a depth of about 10 to 15 meters.

Sonic velocity as a function of porosity for three ranges of calcium carbonate ($CaCO_3$) content (0 to 35 per cent, 36 to 64 per cent, and 65 to 100 per cent) is plotted in Figure 10. The data are compared with two theoretical curves based on an equation of Wood, 1941:

$$V = (K/p)^{1/2}$$

where $1/K = n/K_w + (1-n)/K_g$

$$p = np_w + (1-n)p_g$$

V = velocity

K = bulk modulus

p = density

n = porosity

and subscrips w and g represent liquid and solid fractions, respectively.

For these curves it is assumed that the solid fraction has a compressional wave velocity of 6.0 km/sec, Poisson's ratio of 1/4, and a density of 2.20 g/cm^3 (upper curve) or 2.65 g/cm^3 (lower curve); and that the water has a velocity of 1.53 km/sec and a density of 1.03 g/cm^3. The Wood theory assumes no lattice or shear strength in the aggregate and should represent a lower limit to the actual velocity for a given two phase composition; more reliable for high porosities than for low. Note that both theoretical curves have minima,

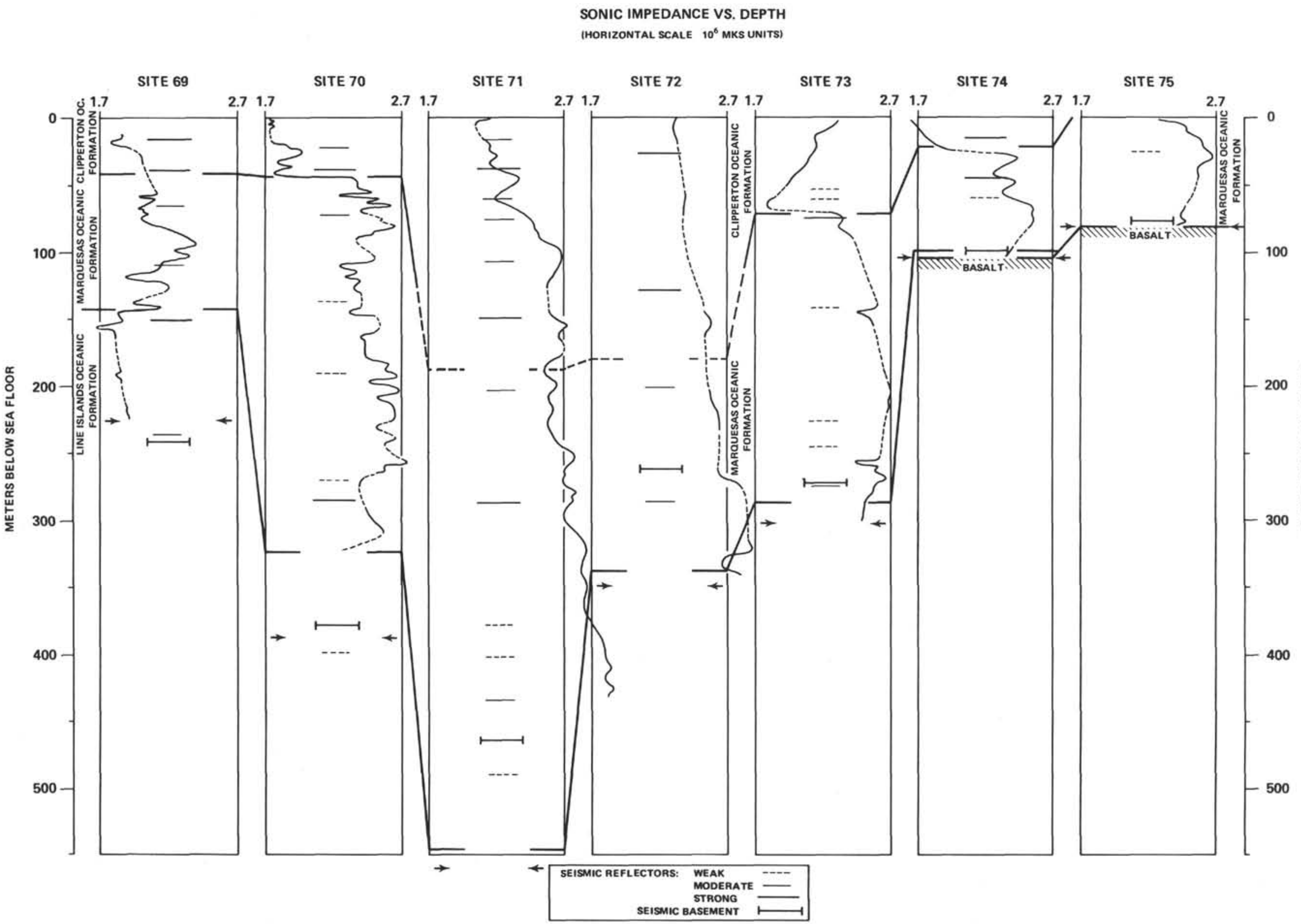

Figure 6. *Sonic impedance (velocity times bulk density) of unlithified sediments compared with depth of seismic reflectors.*

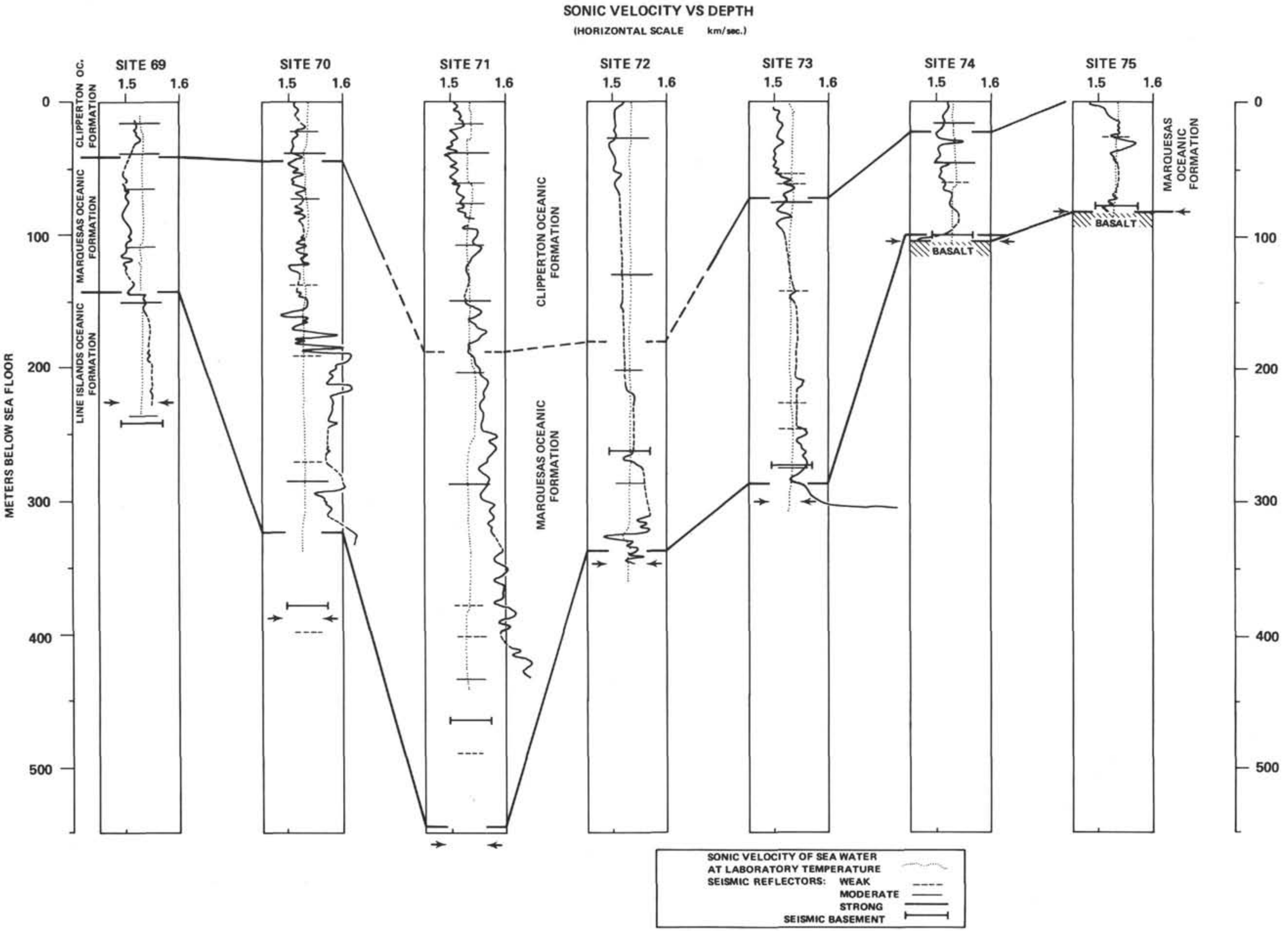

Figure 7. *Sonic velocity of unlithified sediments compared with depth of seismic reflectors.*

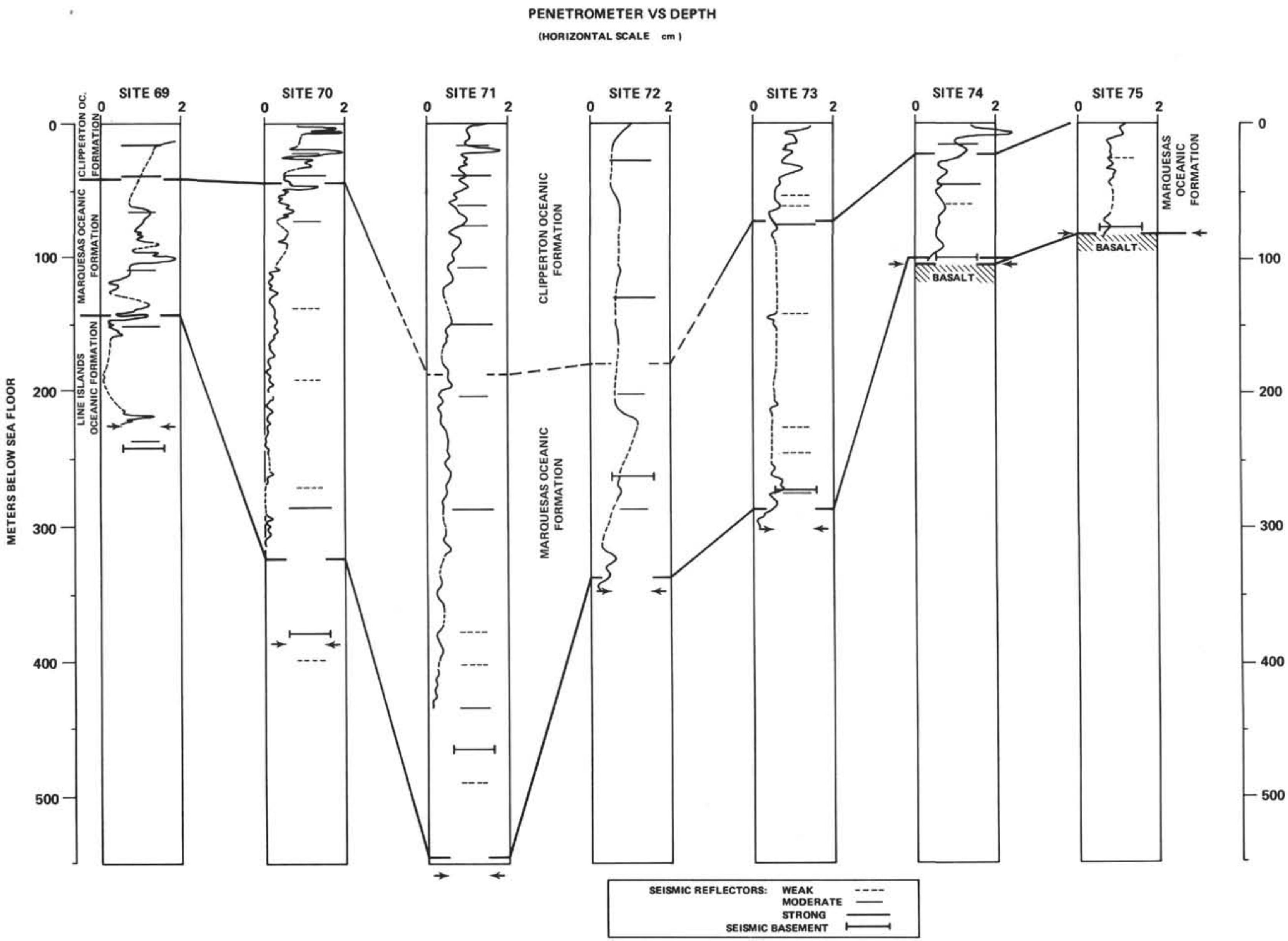

Figure 8. *Penetrability of unlithified sediments compared with depth of seismic reflectors.*

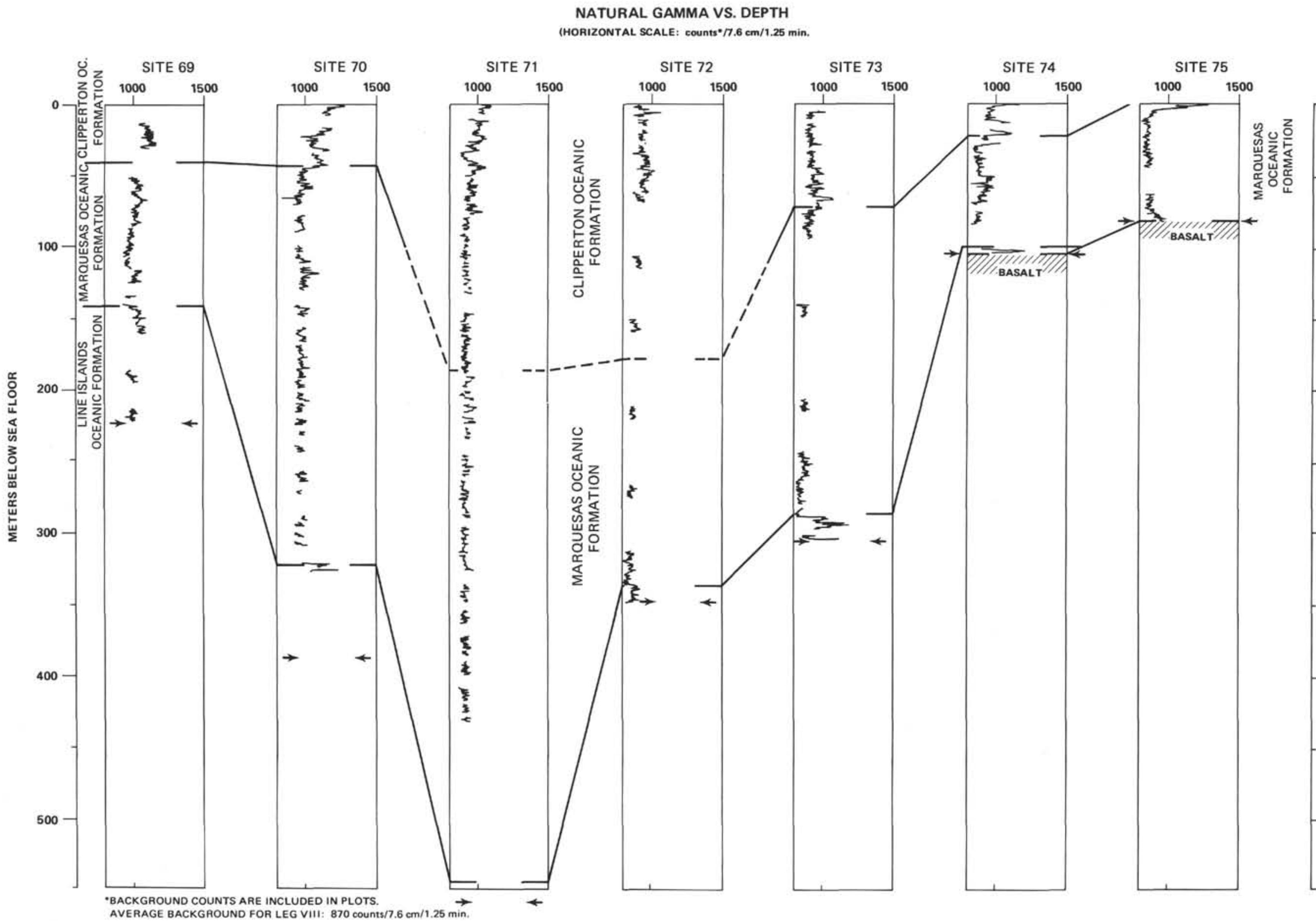

Figure 9. *Natural gamma radiation of unlithified sediments.*

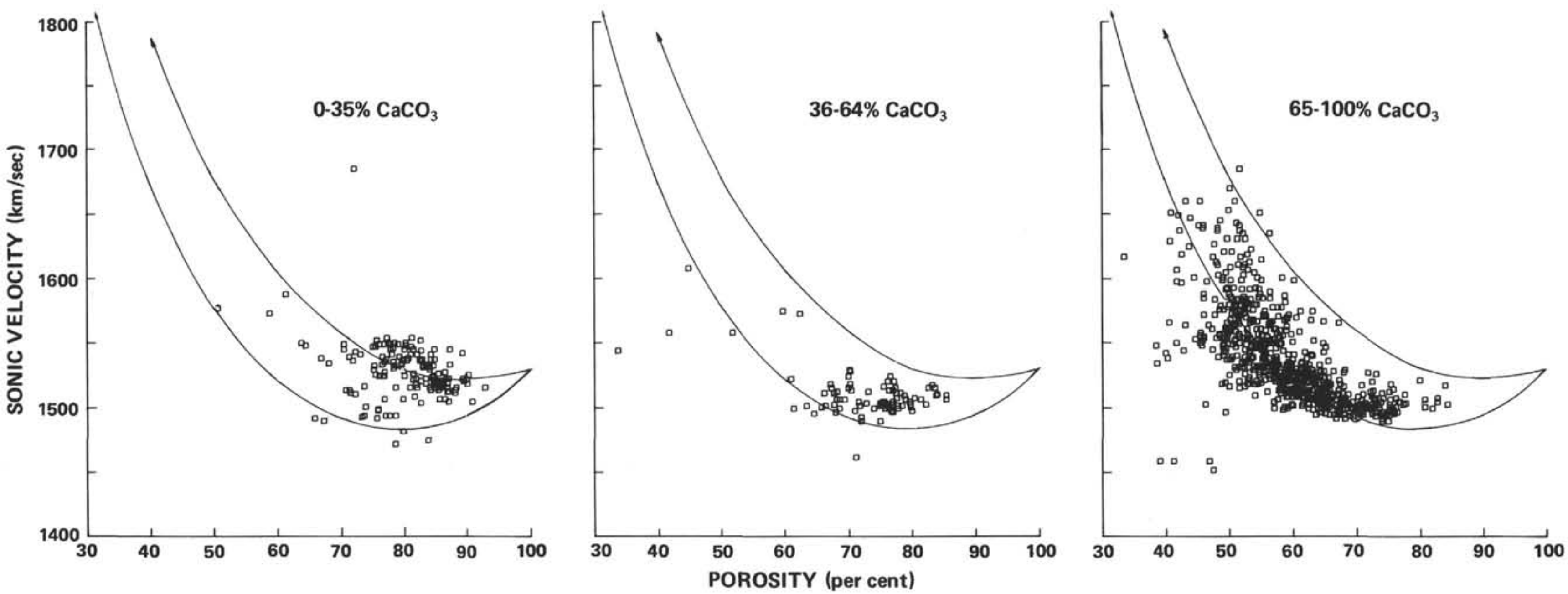

Figure 10. *Sonic velocity versus porosity of unlithified sediments for three ranges of calcium carbonate content. Theoretical curves are based on the equation of Wood (1941). Upper curve, grain-matrix density of 2.2 g/cm^3, appropriate for siliceous ooze. Lower curve, grain-matrix density 2.65 g/cm^3, appropriate for calcareous ooze.*

where the velocity is lower than that for water: near 80 per cent porosity for the 2.65 g/cm^3 material; and 90 per cent porosity for the 2.20 g/cm^3 material.

Most of the sediments encountered on Leg 8 are composed almost completely of the siliceous and calcareous remains of marine organisms, in varying proportions from nearly pure siliceous to nearly pure calcareous composition. The grain densities chosen for the theoretical curves, 2.20 g/cm^3 and 2.65 g/cm^3, are appropriate values for the siliceous and calcareous materials, respectively. Although there is a considerable amount of scatter in the data they are concentrated about the appropriate curves for high and low calcium carbonate ($CaCO_3$) and fall between the curves for intermediate calcium carbonate ($CaCO_3$) content (Figure 10). Some of the anomalously low velocities, especially for lower porosities, are the result either of entrapped gas within the sediment and the attendant reduction of velocity and increase in attenuation, or of gross fracturing within the sediment which can produce water-filled gaps in the sonic ray path. Some additional scatter is the result of experimental error in the porosity measurements.

The large scatter observed for the grain-matrix density (see plots in Chapters 3 through 10) is probably the result of errors in the volume measurement of the small porosity samples used for the determination. For samples of high porosity a relatively small error in volume measurement can produce a large error in grain-matrix density. The average value for grain-matrix density for the highly calcareous sediments is about 2.6 g/cm^3 and for the siliceous sediments is about 2 g/cm^3, as expected. (See especially Site 69, Chapter 4.) The scatter gives in indication of the reliability of the bulk density and porosity values used in determining acoustic impedance (Figure 6) and used in Figure 10, respectively. An additional check on the porosity values used here can be obtained by comparison with porosities measured with the G.R.A.P.E. (Chapters 3 through 10).

Observed porosities range from less than 40 per cent to greater than 90 per cent and observed velocities in the unlithified sediments are less than 1.7 km/sec.

Changes with depth of sonic impedance (pV) and penetrability (related to the rigidity modulus) are the most likely of the physical parameters measured to correlate with reflecting horizons observed on the airgun records. A comparison of the correlation between seismic reflectors and sonic impedance, sonic velocity, and penetrometer reading versus depth (Figures 6, 7 and 8) is in agreement with this expectation. A number of strong reflectors correlate with changes in impedance and, sometimes, with changes in penetrability where there is no appreciable change in velocity. Further discussion of the correlation of seismic reflectors is given in the following section.

Variation with depth of natural Gamma radiation for Sites 69 through 75 is summarized in Figure 9. Similar plots are included in the site reports, Chapters 3 through 10. At most of the sites the radiation is relatively high in the upper part of the sediment column and near the bottom of the cored section. The Marquesas Oceanic Formation is generally marked by low activity, the increase at its upper and lower boundaries generally being quite abrupt. This low activity is attributed to the small amount of 'impurities' in the highly calcareous biogenic sediments of the Marquesas.

Velocity and density were measured on most of the indurated sediment recovered and on the single piece of basalt large enough to obtain reliable measurements using the equipment available on the *Glomar Challenger.* Results are summarized in Table 2 and in Figure 11. Densities were obtained by weighing the samples in fresh water and in air on a modified beam balance under relatively quiet sea conditions. Velocities were obtained by measuring the transit time of an ultrasonic pulse along a measured distance through the samples. Except where otherwise indicated in Table 2 and Figure 11, velocities and densities are believed to be accurate to about ±2 per cent. When the orientation of the sample was known, and when a signal could be detected, velocity was measured both across the core and along the length of the core, representing horizontal and vertical propagation of seismic energy under the ocean bottom.

With only two exceptions (from 25 cases), the velocities measured across-core (horizontal) were higher than along-core (vertical) velocities; in several cases this velocity anisotropy was a factor of 1.5 to 2. Most of the samples were cherts, limestones, or a combination of the two. The few chalks measured exhibited little anisotropy and provided one of the two exceptions noted above. In addition to having a lower velocity, along-core signals were generally more highly attenuated than across-core signals. The cherts and limestones usually exhibited near-horizontal parting planes. A number of samples separated spontaneously along such planes in the laboratory after partial drying. It is unlikely that the anisotropy *in situ,* where the rocks are subjected to vertical compacting pressure and are fully water-saturated, is as great as that measured in the laboratory. However, the measurements strongly suggest that some anisotropy exists under ocean-bottom conditions. The across-core velocities are probably close to actual horizontal velocities while the along-core velocities are probably somewhat lower than vertical velocities.

TABLE 2
Velocities and Densities-Indurated Samples, Leg 8

Sample Description	Propagation[a] Direction	Velocity km/sec	Density g/cm^3
68-2-CC 2 of 2			
#1 Chert		2.85	2.00
#2 Chert thru hard central portion		2.96	1.70-1.80
thru sides coated with mudstone		1.98	
68A-1-CC			
#3 Chert		3.10	2.20
#1 Mudstone		2.05	2.20
#2 Mudstone		1.94	1.80
69-8-CC Chert		3.72	2.00
70A-9-2, 64 cm			
Chert	D	4.17	2.15
10-1 Chert	D	4.34	2.21
	L	3.86	
20-CC Siliceous nannochalk	D	1.65	1.70
	L	1.64	
28-CC Chert	D	3.38	2.07
	L	3.26	
30-#5 Chert	D	3.42	2.07
	(weak signal) L	2.60	
30-#7 Chert	D	3.36	2.08
	(weak beginning) L	2.50	
30-#8 Chert	D	3.06	2.07
	(very weak signal) L	1.44-1.61	
70B-1-1			
#1 Chert, friable	D	3.73	2.11
#7 Chert, friable	D	3.57	2.11
	(weak signal) L	2.53	
#24 Chert, friable	D	3.21	2.06
#25 Chert, friable	D	3.09	2.02
	(weak signal) L	1.58-1.76	
70B-2-1			
#4 Chert, friable	D	3.66	2.16
#16 Chert, friable	D	3.43	2.09
#18 Chert	D	4.53	2.49
	L	5.72	
70B-3-1 #11 Chert, friable	D	2.90	2.01
	(weak signal) L	1.46-1.70	
71-49-Top Black chert w/white	D	4.98	2.52
limestone layer ~0.1" thick	(weak signal) L	3.83	1.89
Thru limestone layer	D	1.86	
CC Chalk	L	1.73	
71A-1-1			
#3 Chalk w/varves; varved portion	D	1.91	1.81
white unbedded part	D	1.87	
#6 Chalk	(low frequency) D	1.66	1.70
	(low frequency, weak signal) L	1.68	
#11 Chalk	D	1.87	1.71
	D	1.76	

TABLE 2 – *Continued*

Sample Description	Propagation[a] Direction	Velocity km/sec	Density g/cm³
71A-2-1			
#1 Limestone	D	3.32	–
	D	2.61	
	D	2.46	
#5 Limestone w/chert	D	3.58	2.26
	D	4.33	
#7 Limestone w/chert	(weak signal) D	4.11	2.38
	D	4.11	
#8C Limestone (green-friable)	D	2.79	2.12
	L	2.38	
#9 Limestone w/chert	D	3.85	2.32
71A-2-2			
#12 Limestone	D	2.93	2.22
71A-3-1			
#3a Limestone	D	2.80	2.21
	L	2.17	
#3b or c Limestone w/chert	D	4.25	2.34
	L	3.16	
#5 Limestone w/chert	D	4.59	2.39
	D	4.23	
#6 Limestone w/chert	D	4.00	2.35
	L	3.11	
#8 Limestone, friable	D	2.67	–
Limestone, friable	D	2.62	
Limestone, more massive	D	2.86	
71A-3-2			
#9 Limestone	D	3.67	2.23
	D	2.86	
#11 Limestone w/chert		–	2.35
#12B Limestone w/chert (blue-gray chert)	D	6.03	2.38
(white-gray-limey)	D	3.98	
#13B	D	2.85	–
	L	2.01	
#15 Limestone w/chert (brown & gray chert)	D	4.48	2.34
#16 Mainly chert	D	6.10	2.55
	L	5.92	
72-7-0			
Bottom Chert w/Limestone	D	4.09	2.49
	(thru limestone) L	3.74	
Top Chert	D	5.03	2.53
	L	4.78	
72-11-1			
#2 Chert	D	3.86	2.29
	L	2.17	
#3 Chert	Near top D	4.02	2.24
	Near bottom D	3.85	
#4 Chert	D	3.76	2.16
	L	2.11	
#5 Chert	D	5.04	2.53
	L	4.20	

TABLE 2 – *Continued*

Sample Description	Propagation[a] Direction	Velocity km/sec	Density g/cm^3
73-21-2 (128-150 cm) muddy limestone	D	1.85	2.01
	D	1.74	
	D	1.79	
73-21-3 (105-117 cm) dark gray chert	D	4.70	2.53
	D	4.65	
74-12-3			
Bottom (1) dark brown indurated carbonate	D	3.89	2.40
& ash	D	3.71	
	L	3.31	
Bottom (2) igneous, black-gray	(3 roughly	6.17	2.89
	orthogonal directions)	6.52	
	(poor coupling, weak, emergent signal)	(5.90)	

[a]D – Along core diameter (horizontal)
L – Along length of core (vertical)

In Figure 11 the velocities and densities are compared with an empirical curve for terrestrial rocks compiled by Nafe and Drake (1963) and with seismically determined velocities for oceanic layers 2 and 3 compiled by Raitt, 1963. For some undetermined reason most of the across-core or unoriented measurements fall above the curve of Nafe and Drake. A number of the chert-limestones fall within or above the range of velocities given by Raitt for layer 2 (velocities above 4.5 km/sec). The basalt sample from Site 74 with an average velocity of about 6.35 km/sec (and a density of 2.89 g/cm^3) falls just below the range of values given by Raitt for layer 3, the oceanic crustal layer.

Thermal conductivity was not routinely measured during Leg 8. Measurements made on sediments from Sites 71 and 72, where determinations of geothermal heat flow were attempted, are given in Chapter 18.

Results of grain size and carbon-carbonate analyses are tabulated in Appendices II and II, respectively.

CORRELATION OF REFLECTION HORIZONS WITH LITHOLOGY

Excellent airgun reflection profiles were obtained throughout most of Leg 8. These are available, along with standard echo sounder and magnetometer records, to aid correlation between sites and to compare conditions at the drilling site with those in the immediate vicinity. A synopsis of reflection records along the *Glomar Challenger* track between Sites 70 and 75 (Figure 14) shows the unconsolidated sediments of the equatorial mound above the acoustic basement. Figure 12 is a summary of reflection records at and near the drilling sites and Figure 13 is a photo-copy of the record across the Clipperton Fracture Zone. Other records and further discussion are included in the Site Reports, Part II, and in Chapter 23, Scan-Challenger Surveys. The acoustic basement on the airgun records corresponds to indurated Eocene sediments at Sites 69, 70, 72 and 73. It is correlated with the top of a thick section of semi-indurated chalk, capped by a 3-centimeter chert layer within the upper Oligocene at Site 71, and is correlated with basalt at Sites 74 and 75.

Acoustic velocities of recovered cores were used to estimate the depths of reflection horizons shown in Figures 6, 7 and 8. At all sites the average vertical velocity throughout the section in unconsolidated or semi-indurated sediments was between about 1.53 km/sec (that of sea water) and 1.6 km/sec (Figure 7). Depth of acoustic basement, using the above mentioned velocities, agrees quite well with the depth of the indurated sediments or basalt in which drilling at the site terminated for Sites 69, 70, 73, 74 and 75. For Site 71 acoustic basement agrees with the bottom of Hole 71 which is the top of a section of lithified chalk containing chert layers that apparently extends down to the Eocene chert and limestone near the bottom of Hole 71A and could act as acoustic basement. At Site 72 acoustic basement is about 80 meters above the bottom of the deeper hole. Steep local dips in basement and errors in location (leaving track passed 300 meters from the beacon) might explain the discrepancy. Nominal basement depth at the site is about 0.1 second (75 to 80 meters) shallower than normal for the vicinity. No improvement in correlation was achieved by using higher velocities.

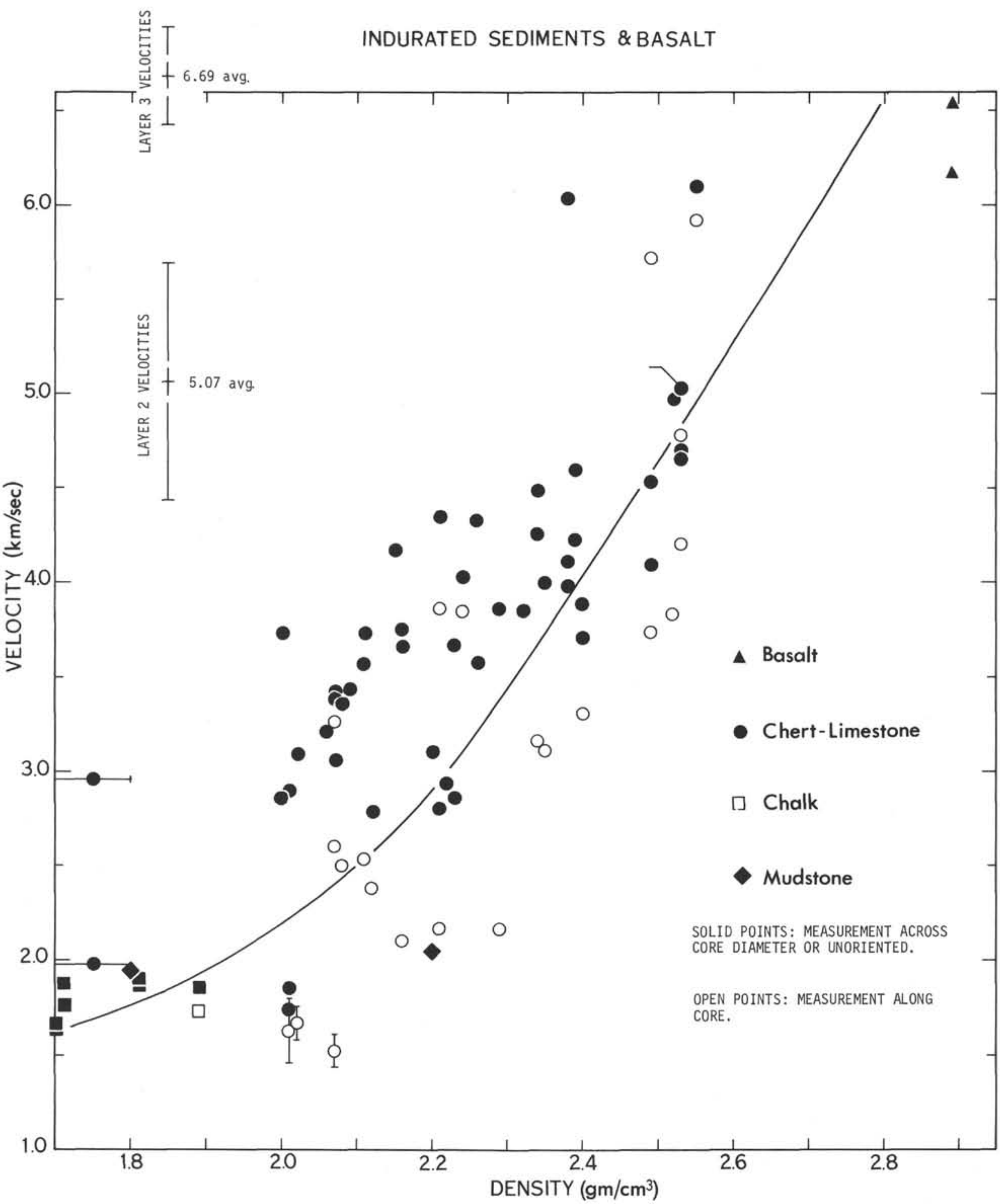

Figure 11. *Compressional wave velocity versus density for indurated sediments and basalt. The curve is an empirical relation obtained by Nafe and Drake, 1963. The velocities shown for oceanic layers 2 and 3 are from Raitt, 1963.*

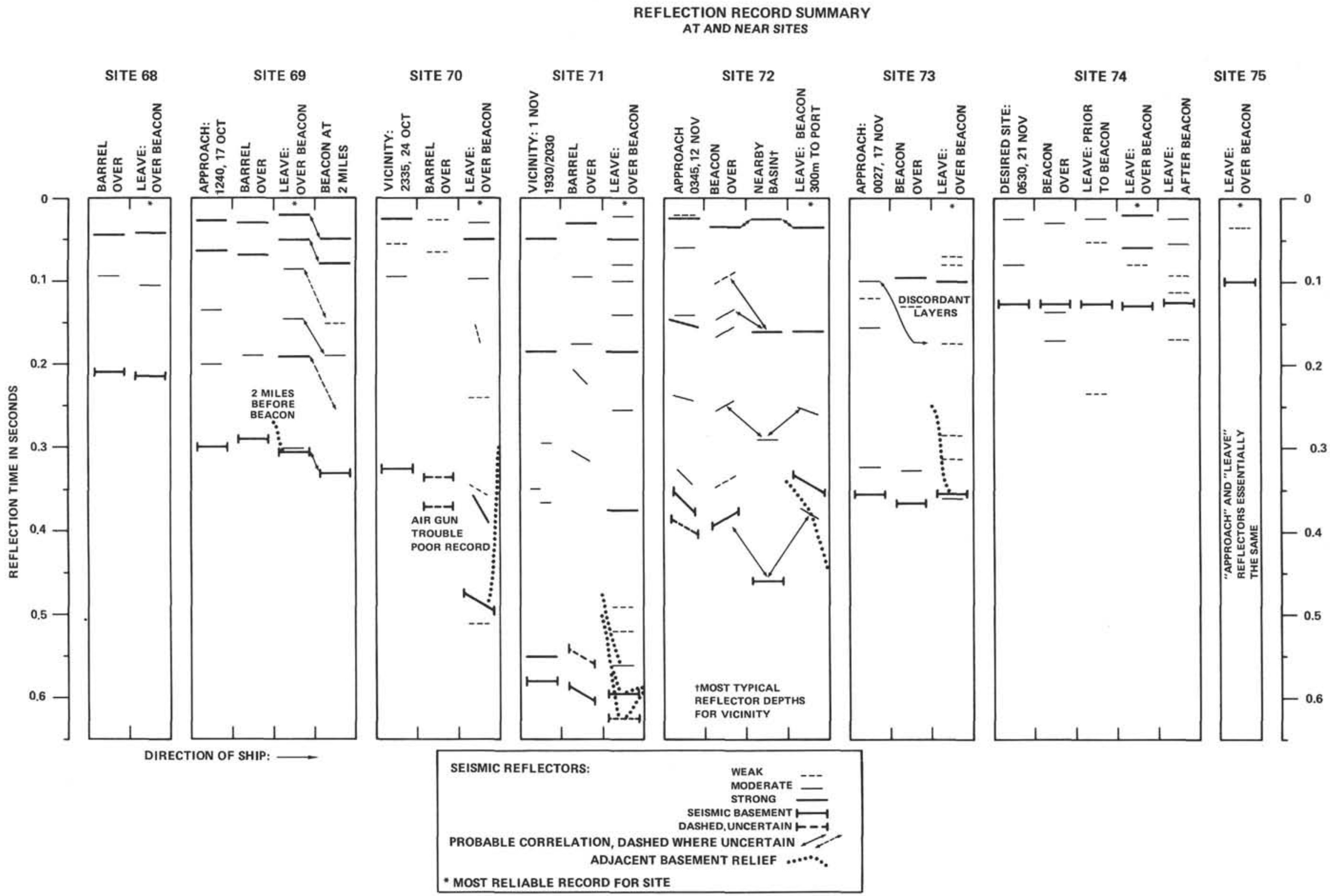

Figure 12. *Summary of seismic reflection horizons near the drilling sites.*

Compressional wave velocities greater than 4.5 km/sec were measured on several samples of limestone and chert, and velocities near 6 km/sec were measured on three chert samples and a basalt sample (Figure 11 and Table 2). These measurements, and the correlations of reflection horizons with prominent lithified sediments or basalts at each site, indicate that "acoustic basement", sometimes considered to be the top of "layer 2" (Raitt, 1963), may vary both in age and in lithology within a region. Basaltic basement therefore may be at an unknown depth beneath a section of lithified sediments and may be difficult to delineate by seismic methods.

The reflection records indicate local structures in the acoustic basement, especially at Sites 70, 72 and 73, that resulted in apparent lengthening or shortening of the sedimentary section at the site relative to that in the neighborhood of the site (Figure 12). Site 70 was drilled over a structural depression or "hole" in the acoustic basement, and the Oligocene part of the section appears to be thicker than normal. Sites 72 and 73 are on the sides of "hills" in the acoustic basement, and the Oligocene part of the section appears to be thinner than that nearby. The sections shown in Figure 16 are the actual recovered thicknesses, but those in Figure 17 have been adjusted to thicknesses typical for the area near the respective drilling sites, using the reflection records as a guide.

The best correlations between intermediate reflection horizons above the acoustic basement and lithologic changes determined by drilling, were observed at Site 69 where the Clipperton and Line Islands Oceanic Formations are highly siliceous and the Marquesas Oceanic Formation is a homogeneous carbonate sequence (Figures 6, 7 and 8). Both the top and bottom of the Marquesas are marked by strong reflections. These two boundaries also appear to be represented in records near Site 70, although the lower reflectors are complicated by local structures. At Site 71, one reflection horizon correlates with the base of the cyclic unit near the top of the Clipperton. At Site 73 a prominent reflector correlates with the Clipperton-Marquesas boundary, which at this location is a sharp contact between nearly pure radiolarian ooze and highly calcareous sediments. The reflector transgresses the section in records near the site, and suggests that the lithologic boundary may be at least locally unconformable. At Site 74 a reflecting horizon correlates with the change from siliceous to calcareous sediments at the base of the Clipperton. Some additional intermediate reflectors appear to correlate with changes in sonic impedance, velocity, or penetrability. Many, however, do not correlate with any obvious lithologic or physical changes.

The assignment of paleontologic ages to sediments cored on Leg 8 is based on the biostratigraphy of three fossil groups: foraminifera, calcareous nannofossils, and Radiolaria—summarized in the preceding chapter and discussed in more detail in Part III of this volume. The absolute ages used for biostratigraphic zones and stratigraphic boundaries are from Berggren (1969) and are shown in Chapter 1, Figure 2.

Preservation of Fossils

Calcareous nannoplankton form the major constituent of all carbonate-rich sediments sampled on Leg 8. The preservation of these microfossils is generally good in the upper Oligocene through Pliocene parts of the section at Sites 71, 72 and 73, but solution and recrystallization are common in samples from the upper Eocene through the lower Oligocene, and from the Quaternary. Foraminifera are generally a minor component of the calcareous sediments. The marked scarcity of fragile planktonic forms such as *Globigerinoides* and *Orbulina* indicates selective solution of the assemblage. These shells commonly show solution in almost all parts of the stratigraphic section.

Radiolaria are usually the most abundant siliceous microfossils in the sediments although diatoms are common to abundant in the lower Oligocene and in the upper Miocene to Quaternary interval. The preservation of siliceous tests is consistently good in the middle Miocene through the Quaternary. In the lower Miocene, preservation varies from poor at the southern Sites 74 and 75 to good at Site 70 in the north. Oligocene faunas commonly show marked signs of solution, and they have been totally dissolved in the southern sites.

The degree of preservation of all fossil groups is generally related to the rate of sediment accumulation. For a given stratigraphic interval, both calcareous and siliceous microfossils are best preserved at sites where this interval is represented by the thickest section. The patterns of distribution of calcareous and siliceous microfossils, however, are not identical, nor are they constant with time.

Prior to the early Miocene, sediments containing both siliceous and calcareous microfossils were deposited at Site 42 at 13° 51'N. At this time the southern boundary of opal-rich sediments lay between Sites 73 and 74, at about 4°S, whereas calcareous deposits were accumulating at Site 75 at about 12°S. This pattern changed during early and middle Miocene time, and from about late Miocene time to the present the northern boundary of sediments rich in opaline silica has been between Sites 70 and 42, at about 10°N, and the southern boundary has been between Sites 74 and

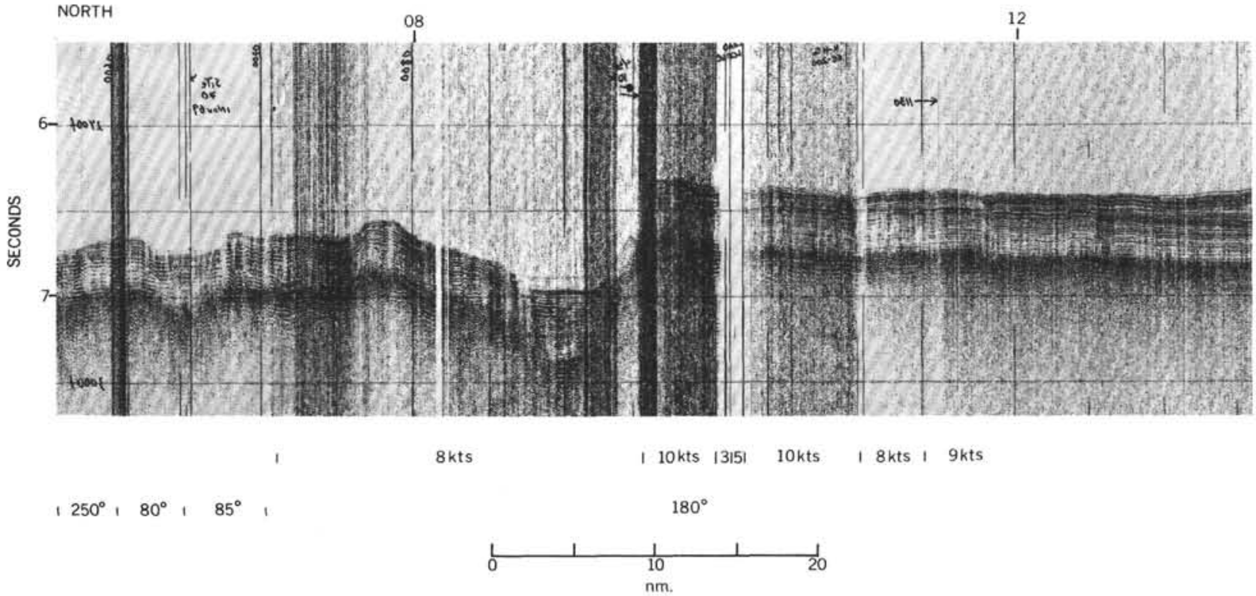

Figure 13. *Airgun record across Clipperton Fracture Zone.*

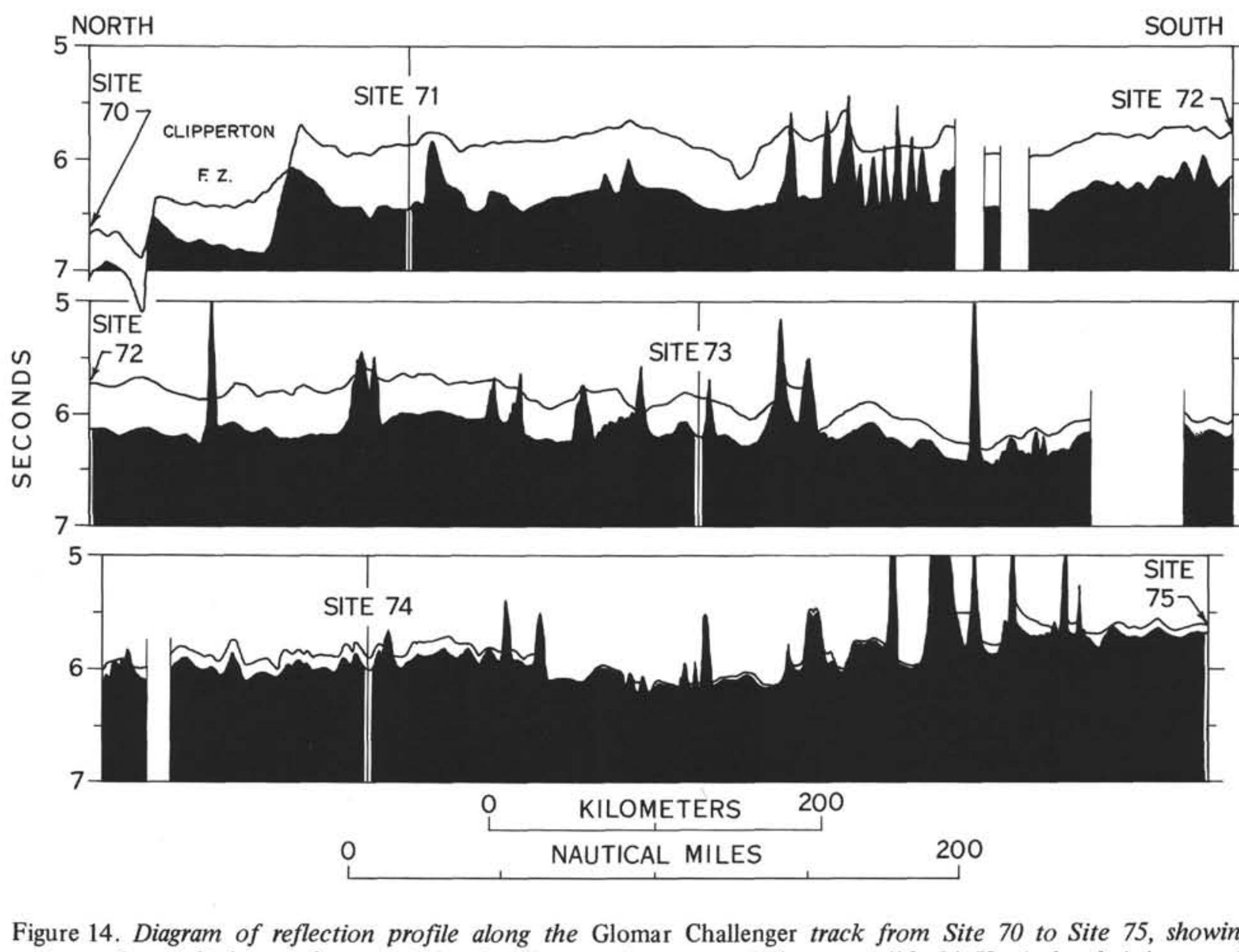

Figure 14. *Diagram of reflection profile along the* Glomar Challenger *track from Site 70 to Site 75, showing approximate thickness of unconsolidated sediments above acoustic basement (black). Vertical scale is in seconds travel time, horizontal scale is not uniform between sites.*

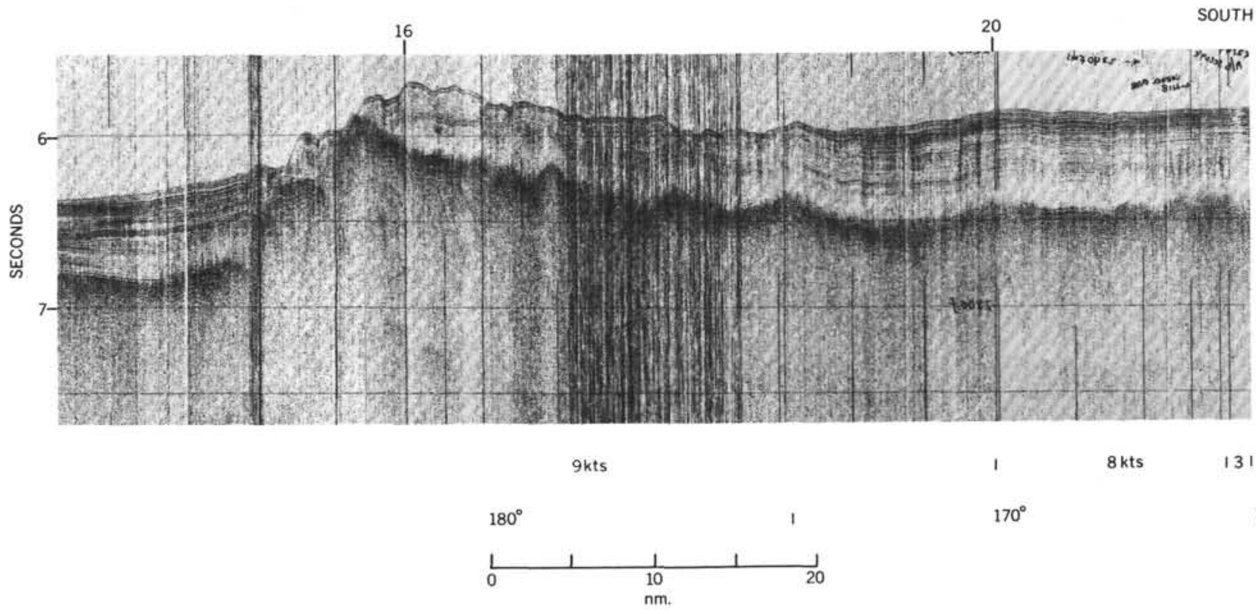

Figure 13. *Continued.*

75, at about 10°S. The limits of calcareous deposition from late Miocene to the present are approximately 5°N to 5°S.

Thus, the latitudinal extent of calcareous microfossils considerably exceeded that of the siliceous microfossils during Oligocene into early Miocene time. Since that time the extent of calcareous microfossils has diminished whereas that of the siliceous microfossils has exceeded that of the calcareous microfossils since about late Miocene time.

Breaks in the Stratigraphic Record

Reworking and hiatuses are present at most sites. Some of these disturbances in stratigraphic order may be local, but in all sections cored two intervals are repeatedly marked by reworking of older microfossils and by breaks in the stratigraphic record: the middle Eocene to lower Oligocene and the lower Miocene to lower Pliocene. Prominent hiatuses and the lithology at each site are shown in Figure 15.

The Eocene-Oligocene (Line Islands-Marquesas) boundary is a disconformity and is usually marked by a sharp lithologic change. Faunal and floral hiatuses commonly occur just above and below this boundary as well.

The nature of the disturbance in the lower Miocene to lower Pliocene (Marquesas-Clipperton) varies with the rate of sediment accumulation. At sites with high rates of accumulation (71 and 72), some reworking of older microfossils is present in the upper Miocene and lower Pliocene. To the north and south at sites with intermediate rates of accumulation (70, 73, 74) intensive reworking, short hiatuses, and possible unconformities are found. At the fringes of the high productivity region (Sites 42 and 75), long hiatuses extending from the lower Miocene to the Quaternary bring the lower and middle Cenozoic sections within a few meters of the sea floor. The specific causes for some of these breaks in the record and for the reworking of older sediments may be due to relatively local tectonic events, but it appears that they reflect more general changes that occurred throughout the Pacific during Miocene time.

Sediment Accumulation Rates

The lithologic cross section shown in Figure 4 indicates the distribution of sediments during the Cenozoic, and the average accumulation rates for each epoch at each site are shown in Figure 16. (Figure 6 in each of the Site Reports (Chapters 3-10) is a plot of age versus depth based on the biostratigraphic zonations of the foraminifera, nannoplankton, and Radiolaria, with the time scale in millions of years based on that of Berggren (1969).) It is difficult, however, to interpret changes in sedimentation and sediment accumulation rates during short, discrete segments of geologic time. By relating our stratigraphic studies to the revised time scale of Berggren (1969), a "thickness of accumulated sediment" can be determined for any sampled period of geologic time (Figure 17). Choosing segments of time which are both equal and short (5 million years) results in a detailed picture (within the context of this time scale) of sediment accumulation in the equatorial Pacific from Oligocene time to the present. The drilled intervals at Sites 70, 72 and 73 were adjusted using

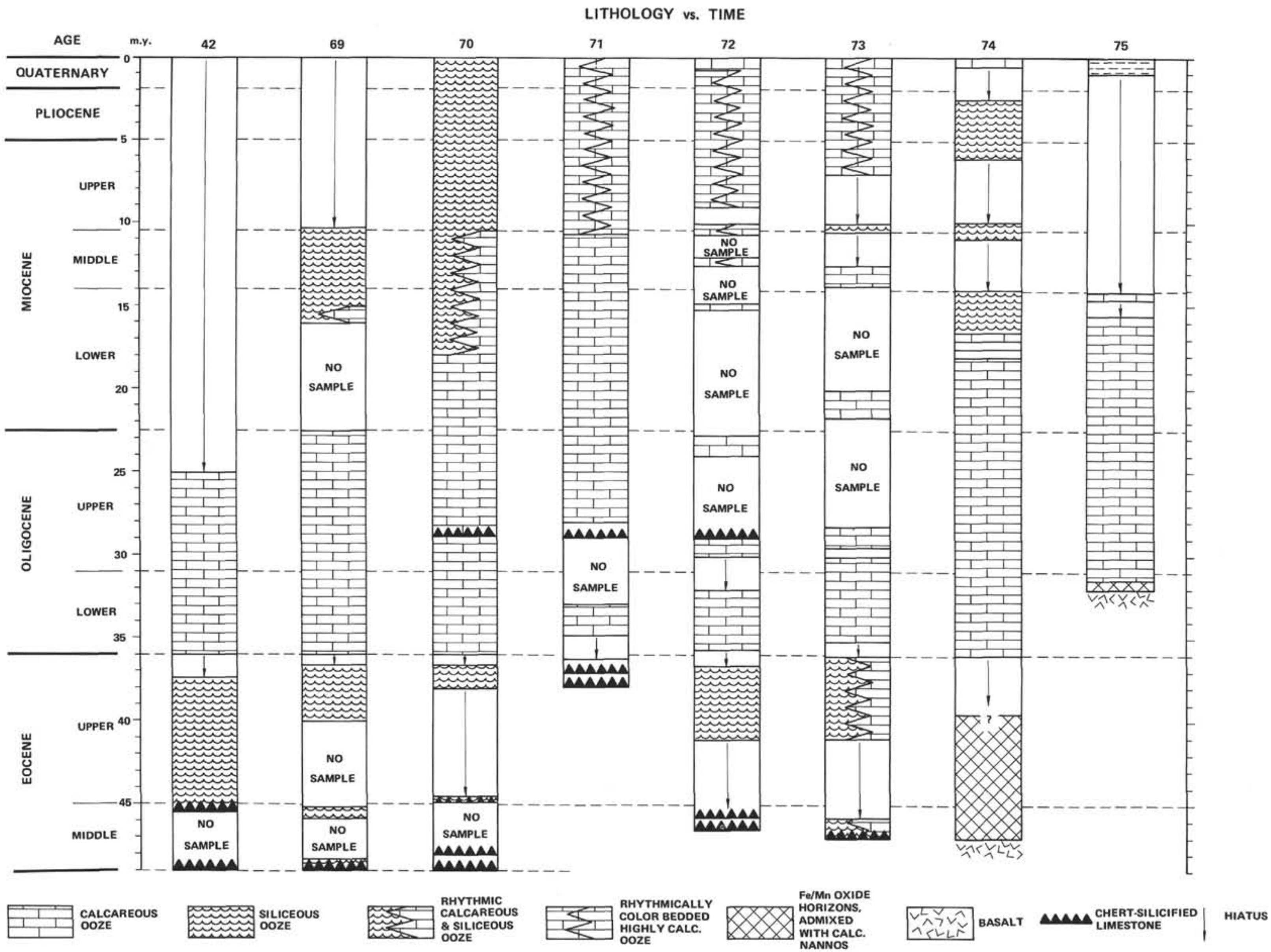

Figure 15. *Comparison of lithology versus time for Site 42 from Leg 5 and Site 69 through 75 of Leg 8.*

STRATOGRAPHIC SUMMARY

SITE / DURATION M.Y.		68 Boundary†	*	69	*	70	*	71	*	72	*	73	*	74	*	75	*
QUATERNARY	2		0.1		0		1.5		4.5		8.5		7.5		0		0.5⁻
		0.2				3⁻		9±2		$17\pm^{1}_{2}$		$15\pm^{5}_{1}$				1⁻	
PLIOCENE	3						1.5		3.0		11.7		13.3		3.3		
						7.5±1		18±2		52±2		$55\pm^{5}_{3}$		11±2			
UPPER MIOCENE	5.5						2.3		7.5		11.1		3.1		0.9		
						20±3		59±2		113±3		72±3		16			
MIDDLE MIOCENE	3.5				8.0		5.7		33.1		16.3		9.4		0.6		
				28±10		40±5		175±5		170±20		105±10		18			
LOWER MIOCENE	8.5				2.8		8.6		20.2		10.6		8.8		2.6		3.9
				$52\pm^{10}_{12}$		113±10		347±5		260±10		180±20		40±3		34±4	
UPPER OLIGOCENE	8.5				8.8		18.0		18.0		8.2		8.2		5.1		4.4
				127±10		$266\pm^{5}_{20}$		500±15		330±5		250±5		83±3		71±3	
LOWER OLIGOCENE	5				3.4		11.6		9.0		2.0		7.6		3.4		
				144±10		324±3		545±6		340±3		288±2		100			
UPPER EOCENE	9				4.0		1.2						1.3		0.1		
				180±10		$335\pm^{6}_{30}$						300±3		101±1			
MIDDLE EOCENE	4																
		14.8															

† BOUNDARIES (meters below sea floor)

* SEDIMENTATION RATES (meters/m.y.)

Figure 16. ***Stratigraphic summary showing depth below sea floor to stratigraphic boundaries in meters, and average sedimentation rates for each epoch, in meters per million years. Duration of epochs, in millions of years, after Berggren (1969).***

profiler records to make the sediment thicknesses representative of the average thickness of the regions in which these three holes were drilled. In addition, sediment thicknesses for all sites were corrected for differential compaction by standardizing to a porosity of 50 per cent, and the profiles were plotted as individual, simplified cross sections. A consideration of this sequence of profiles together with the stratigraphic information summarized in Figures 4, 5, 15 and 16, leads to the following generalizations concerning the development of the equatorial band of pelagic sediments:

1. The region of highest sediment accumulation rate has been centered on or near the equator from late Miocene time to the present. During middle and early Miocene time the axis of this zone was 3 to 5 degrees north of the equator, and the Oligocene axis was perhaps even further north. Information on Eocene accumulation rates is insufficient to define the axis at this time.

2. Over the latitudinal extent of the cross section, sediment accumulation rates were generally 2 to 4 times greater during the late Oligocene to middle Miocene time than during the Pliocene and Pleistocene. If we look at the individual sites, however, the rates of accumulation are to increase through the Oligocene, but drop sharply during the early Miocene at the peripheral Sites 42, 70, 74 and 75; whereas, at the central sites they continue to increase through the middle Miocene at Site 71, and are relatively high through the Pliocene at Sites 72 and 73.

3. The equatorial zone of highly fossiliferous calcareous sediments was much broader during Oligocene and early Miocene time than later. At longitude 140°W, the zone spanned more than 25 degrees of latitude during Marquesas deposition, whereas it covered less than half of that during Clipperton deposition.

4. Comparable intervals of the Clipperton Oceanic Formation show distinct differences in composition (facies) and in thickness between Sites 70 and 71 across the Clipperton Fracture Zone at 5°N, and account for about a hundred meters of the apparent displacement (Figure 13). Comparable intervals of the Marquesas Oceanic Formation show little difference in composition or in actual uncorrected thickness of sediment (Figure 4) across the Clipperton Fracture Zone, although too little of the lower Oligocene was cored at Site 71 for accurate comparison of composition, or of the effects of solution and lithification. If the sections are corrected for the apparent abnormal thickness of Oligocene sediments at Site 70, which the seismic profiles indicate, the upper Oligocene sediments are significantly thinner north of the Clipperton Fracture Zone (Figure 17). Differences in lithology and in the uncorrected thickness between Sites 70 and 71 thus suggest major vertical displacement on the Clipperton Fracture Zone during early Miocene time, whereas comparison of the corrected thicknesses (Figure 17) suggests that significant vertical displacement may have occurred in Oligocene time.

DISCUSSION

The differences in composition and diagenesis, and the widespread disconformity between the Line Islands and Marquesas Oceanic Formations suggest major changes in oceanic circulation and geochemistry between the Eocene and Oligocene. Interpretation of these changes is hindered by the lack of continuous core in Eocene sediments.

We can make no interpretation of the amount or rate of sea floor movement from the drilling results, inasmuch as the line of holes is more or less normal to the major fracture zones and to the probable direction of plate movement in the region, and because basaltic rock was cored at only two sites, 74 and 75. That at Site 74 was overlain by thin sediments of Eocene age, possibly the top of the middle Eocene; and that at Site 75 was overlain by sediments of early but not earliest Oligocene age. Both sites are not far from the base of the Marquesas Islands Ridge, and the basaltic rock at one or both sites may be associated with early formation of the Marquesas Ridge rather than with the East Pacific Rise.

The high rate of sediment accumulation during Oligocene and Miocene time was accompanied by widespread deposition of sediments rich in calcareous nannoplankton, and indicates that during this time either productivity was greater than at present, or solution of carbonate tests during and after deposition was less than at present. The occurrence in the Pacific of calcareous Oligocene and lower Miocene sediments at depths below the present carbonate compensation depth indicates that the compensation depth was perhaps deeper during these epochs than at present (Heath, 1969) or alternatively that the sea floor was shallower. Information from the Leg 8 drilling is insufficient to determine whether the high accumulation rates and great lateral extent of the lower and middle Cenozoic sediment resulted from a shallower sea floor, a very deep lysocline[4] (Berger, 1970) or a weak lysocline (a low rate of solution), a high rate of production, or perhaps a combination. The effective result was a deeper compensation depth and thicker and more widely distributed fossiliferous sediment.

The variations in lateral extent and thickness of the equatorial band of sediments at different times during the Cenozoic account for the location of the axis of the cumulative equatorial mound of sediments at about

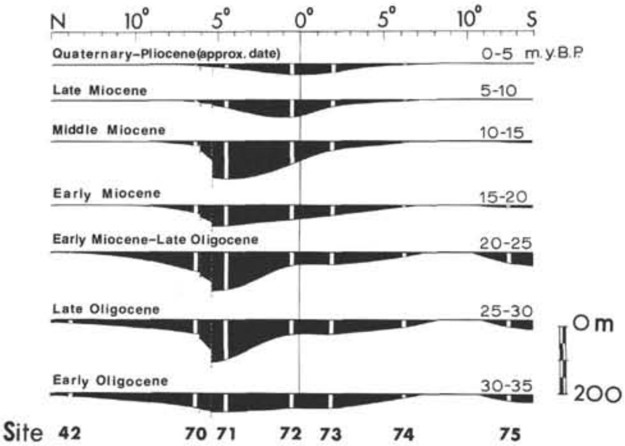

Figure 17. *Idealized cross sections of accumulated sediment thickness in 5 million year increments. Approximate stratigraphic age of each increment is given on the left side of the sections. Ages on the right side of each section are in millions of years before present (Berggren, 1969). Site locations are shown on cross sections as vertical white lines and are numbered at the bottom of the figure. Thickness of sediments has been corrected to 50% porosity, and also adjusted to average thickness of sediments around each site by using seismic profiler records. The Clipperton Fracture Zone between Sites 70 and 71 is shown by vertical dashed lines. The area of nondeposition between 7°S and 10°S is east of the Marquesas Islands.*

3°N at this longitude (Figure 2), whereas the thickest part of the Pliocene and Quaternary sections is at or just south of the Equator. This change in position of the axis of most rapid sediment accumulation and the southward migration of opal-rich sediments could have resulted from at least two different causes: a change in the pattern of divergence and circulation in the equatorial Pacific, as might be expected in the early Cenozoic when high latitude and bottom water temperatures were higher (Emiliani, 1966, Lipps, 1970) and the isthmus of Panama, northern Colombia, and Venezuela were a seaway (Whitmore and Stewart, 1965; Woodring, 1966); or a migration of the sea floor due to sea floor spreading (Pitman *et al.*, 1968).

If sea floor spreading were the main cause of the change in position of the axis of most rapid sediment accumulation (Hayes *et al.*, 1970), the displacements seen in Figure 17 would require a strong northerly component of motion of the sea floor, especially in the middle and late Miocene. If the apparent rise in compensation depth after early Miocene time were caused by a deepening of the sea floor as it migrated away from the spreading center, there should be a

[4]The lysocline is the level below which solution of carbonate increases rapidly–about 4000 meters in this region. The calcium carbonate compensation depth is the level at which the rate of solution balances the rate of supply–approximately 4500 meters in this region.

gradual change in composition of the sediments rather than the marked changes from Marquesas to Clipperton deposition seen at Sites 69, 70, 73, 74 and 75.

The change from Marquesas to Clipperton deposition in the stratigraphic section (Figures 4, 5 and 16) shows a marked constriction of the broad band of carbonate sediments to a relatively narrow equatorial band, an increasing rate of sediment accumulation at near-equatorial sites through the middle Miocene (Site 71) and Pliocene (72, 73) together with sharply decreasing rates and increasing solution at outer sites (69, 70, 74, 75), and the change from steady sedimentation in the Marquesas to variable or cyclic deposition in the Clipperton—starting in early to middle Miocene time. The change is also marked by disconformities, faunal hiatuses, and intensive reworking of sediments.

These observations indicate that a major change in oceanic circulation began in early Miocene time which resulted in intensification of equatorial currents and divergences. At about the same time, local and regional tectonic events coincided with the onset of tectonic activity around the Pacific Basin summarized by Dott (1969), and with the episodes of emergence of atolls in the Central Pacific shown by the drilling of Bikini, Eniwetok and Midway (Schlanger, 1963; Hsu and Schlanger, 1968); Ladd and others, 1970).

The Central America seaways were open in Oligocene time and a land bridge had formed by the late Pliocene (Whitmore and Stewart, 1965). Crowell and Frakes (1970) suggest that the onset of Cenozoic glaciation may be related to changes in Pacific oceanic circulation patterns, from meridional to latitudinal, caused by closing of the seaways in Pliocene time. Recent evidence indicates that major glaciation was present in Alaska at least 10 million years ago, and in Antarctica at least 7 million years ago (Denton and Armstrong, 1969; Rutford and others, 1970).

Thus two factors, possibly interrelated (Crowell and Frakes, 1970) may account for the changes observed in the equatorial sedimentary formations. (1) Miocene tectonic activity may have restricted flow through the Central America seaways before they were closed off in Pliocene time, thus changing equatorial Pacific circulation patterns. (2) An intensification of the vertical and horizontal oceanic thermal gradients, as indicated by glaciation in polar regions, would also intensify atmospheric and oceanic circulation patterns (Lipps, 1970).

More precise interpretations of the Cenozoic history of the equatorial current system derived from the distribution of sediments, as suggested by Arrhenius (1963), will require far more detailed mapping of the formations proposed here and of their subdivisions. The mapping in many places can be carried out using the normal coring techniques of marine geology, as has already been done at reconnaissance scales by Hays and others (1969). Also, of course, more closely spaced drill holes along this and other equatorial sections will be needed for more precise definition of the shifting facies of siliceous and carbonate sediments that record the history of the equatorial currents.

REFERENCES

American Commission on Stratigraphic Nomenclature, 1961. Code of stratigraphic nomenclature. *Bull. Am. Assoc. Petrol. Geologists.* **45**, 645.

Andrews, J. and Hsu, K. J., 1970. Stratigraphic Commission, Note 38-A, recommendation to the American Commission on Stratigraphic Commission concerning nomenclatural problems of submarine formations. *Bull. Am. Assoc. Petrol. Geologists.* **54**, 1746.

Arrhenius, G. O. S., 1963. Pelagic sediments. **In** *The Sea.* M. N. Hill (Ed.). New York (John Wiley and Sons) **3**, 655.

Berger, W. H., 1970. Planktonic foraminifera: selective solution and the lysocline. *Marine Geology.* **8**, 111.

Berggren, W. A., 1969. Cenozoic chronostratigraphy, planktonic foraminiferal zonation and the radiometric time scale. *Nature.* **224**, 1072.

Bramlette, M. N., 1961. Pelagic sediments. Oceanography. *Am. Assoc. Advan. Sci. Publ.* **67**, 345.

Cromwell, T., 1953. Circulation in a meridional plane in the Central Equatorial Pacific. *J. Marine Res.* **12**, 196.

Crowell, J. C. and Frakes, L. A., 1970. Phanerozoic glaciation and the causes of ice ages. *Am. J. Sci.* **268**, 193.

Denton, G. H. and Armstrong, R. L., 1969. Miocene-Pliocene glaciations in southern Alaska. *Am. J. Sci.* **267**, 1121.

Dott, R. H., Jr., 1969. Circum-Pacific late Cenozoic structural rejuvenation: implications for sea floor spreading. *Science.* **166**, 874.

Emiliani, C., 1961. The temperature decrease of surface sea-water in high latitudes and of abyssal-hadal water in open oceanic basins during the past 75 million years. *Deep-Sea Res.* **8**, 144.

Ewing, J., Ewing, M., Aitken, T. and Ludwig, W. J., 1968. North Pacific sediment layers measured by seismic profiling. The crust and Upper Mantle of the Pacific. *Trans. Am. Geophys. Union.* Mon. 12, 147.

Graham, H. W., 1941. Plankton production in relation to character of water in the open Pacific. *J. Marine Res.* **4**, 189.

Hays, J. D., Saito, T., Opdyke, N. D. and Burckle, L. H., 1969. Pliocene-Pleistocene sediments of the equatorial Pacific: their paleomagnetic biostratigraphic and climatic record. *Bull. Geol. Soc. Am.* **80**, 1481.

Heath, G. R., 1969. Carbonate sedimentation in the abyssal equatorial Pacific during the past 50 million years. *Bull. Geol. Soc. Am.* **80**, 689.

Hsu, K. J. and Schlanger, S. O., 1968. Thermal history of the upper mantle and its relation to crustal history in the Pacific Basin. *Proc. XXIII Intern. Geol. Congr.* **1**, 91.

Ladd, H. S., Tracey, J. I. and Gross, M. G., 1970. Deep drilling on Midway Atoll. *U. S. Geol. Surv. Profess. Paper.* 680-A.

Lipps, J. H., 1970. Plankton evolution. *Evolution.* **24**, 1.

McManus, D. A., *et al.,* 1970. *Initial Reports of the Deep Sea Drilling Project, Volume V.* Washington (U. S. Government Printing Office).

Nafe, J. E. and Drake, C. L., 1963. Physical properties of marine sediments. **In** *The Sea.* M. N. Hill (Ed.) New York (John Wiley and Sons) **3**, 794.

Pitman, W. C., III, Herron, E. M. and Heirtzler, J. R., 1968. Magnetic anomalies in the Pacific and sea floor spreading. *J. Geophys. Res.* **73**, 2069.

Raitt, R. W., 1963. The crustal rocks. **In** *The Sea.* M. N. Hill (Ed.) New York (John Wiley and Sons) **3**, 85.

Reid, J. L., 1962. On circulation, phosphate-phosphorous content, and zeoplankton volumes in the upper part of the Pacific Ocean. *Limnol. Ocean.* **7**, 287.

Riedel, W. R. and Funnell, B. M., 1964. Tertiary sediment cores and microfossils from the Pacific Ocean floor. *Quart. J. Geol. Soc. London.* **7**, 305.

Rutford, R. H., Craddock, C. and Bastien, T. W., 1968. Late Tertiary glaciation and sea-level changes in Antarctica. *Paleogeogr., Paleoclimatol., Paleoecol.* **5**, 15.

Ryther, J. H., 1963. Geographic variations in productivity. **In** *The Sea.* M. N. Hill (Ed.) New York (John Wiley and Sons) **2**, 347.

Schlanger, S. O., 1963. Subsurface geology of Eniwetok Atoll. *U. S. Geol. Surv. Profess. Paper.* 260-BB.

Whitmore, F. C., Jr. and Stewart, R. H., 1965. Miocene mammals and Central American seaways. *Science.* **148**, 180.

Wood, A. B., 1941. *A Textbook of Sound.* G. Bell and Sons.

Woodring, W. P., 1966. The Panama land bridge as a sea barrier. *Proc. Am. Phil. Soc.* **110**, 425.